Fatigue—A Test Integrated Damage Modeling Approach

Darrell Simpkins,* Robert L. Neulieb,* and Dennis J. Golden†
Air Force Flight Dynamics Laboratory, Wright-Patterson Air Force Base, Ohio

Empirical damage models were developed using the method of least squares and flight simulation test results. The experimental data were obtained from notched coupon specimens subjected to a number of simulated transport flight-by-flight test sequences of alternate loading intensities. Clipping of maximum load levels was performed during test to isolate the influence of load induced microplasticity from the combined influence of micro and macroplasticity on test life. The resulting test data were indicative of load sequence effects resulting from microplasticity at material and fabrication defects contained within a local volume of material adjacent to a notch. Since the specimen was the damage integrator, the resulting models were considered to statistically account for load sequence effects in the development and coalescing of crack nuclei in forming a predominant propagating crack. Results indicate that the models present a viable alternative to the Palmgren-Miner approach.

Nomenclature

f_{1g} = flight 1-g trim stress, KSI
$f_{\min}$ = minimum ground stress, KSI
n = cycles per flight, number of cycles
σ^2 = mean square value, KSI^2
Δf = incremental flight stress, KSI
Δg = incremental vertical load factor
Σ = summation, cumulative occurrences
N = cycles to rupture, damage index
Z = ratio of $f_{\min}$ to f_{1g}
g = vertical load factor
f_m = cycle mean stress, KSI
f_a = cycle alternating stress, KSI
(n/N) = cycle ratio
K_t = theoretical stress concentration

Subscripts

ac = actual
d = desired

Introduction

THE Palmgren-Miner linear damage theory[1] and constant amplitude *(S-N)* fatigue data are inadequate for consistently predicting the mean life of test specimens which are subjected to simulated flight-by-flight sequences (see Fig. 1 for a sample segment of these sequences) with randomly ordered loads.[2] Among the possible reasons for this inadequacy, we recognize that load induced plasticity, both on the micro and macro level, can lead to nonlinear accumulation of fatigue damage. For example, load induced residual stresses may be beneficial in lengthening laboratory specimen lives, but the relaxation of these stresses is not well understood and must be studied further in order to properly model its influence. This aspect is discussed in later sections of this paper.

Received January 28, 1974; revision received May 24, 1974. The authors wish to acknowledge the efforts of The University of Dayton Research Institute in accomplishing the experimental phase of this work. They particularly wish to thank G. J. Roth of the Institute for his contributions to the experimental phase. The authors also wish to acknowledge the efforts of the Analog/Hybrid Computation Branch, 4950/ADS, Wright-Patterson AFB, Ohio in converting digital tapes to continuous analog signals suitable for recording on an FM recorder. In particular, the authors wish to thank F. W. Kasischke for his contribution.

Index categories: Aircraft Structural Design (Including Loads); Materials, Properties of; Aircraft Structural Materials.

*Aerospace Engineer, Structural Integrity Branch, Structures Division.

†Major, USAF, Principal Scientist, Structural Integrity Branch, Structures Div.

While we feel that there is a potential for analytically calculating the plastic stresses on a macro level and their influence of modifying notch cyclic stress levels, the effects of plasticity at the micro level is much less understood. It was decided that the effects of plasticity at the micro level could best be accounted for statistically. Therefore, in this investigation, only loads that would induce microplasticity (no significant macroplasticity) were included in the fatigue test load sequences. The test specimen, which is assumed to include defects acting as stress risers at the micro level, is viewed as a damage integrator accounting for the effect of loading sequence on test life. It is hypothesized that the integration process consists of strain accumulation through microcrack formation and extension from defects. The strain accumulation rate is nonlinear, and it is influenced by load interaction effects arising from both the higher and lower loads within a sequence as well as microcrack length. Several specimens were tested to each of several alternate intensity flight-by-flight sequences so that a representative number of defects and the response of these defects to simulated flight-by-flight cyclic loads were included in a data base for damage modeling. Additional tests were made to provide data to evaluate the proposed test integrated damage models.

In this investigation, two models are developed and evaluated. One model (referred to as the sequence model) is based on the concept that damage is accumulated by a load amplitude sequence and that there are parameters which characterize the sequence and identify the sequence damage. The second model (referred to as the cycle-by-cycle model) is based on linear summation of damage on a cycle-by-cycle basis as in Miner's rule but differing in that the model is based on simulated flight-by-flight fatigue tests.

The investigation includes 1) establishing load truncation levels for laboratory simulation test and, 2) the generation of fatigue life allowables such that the test specimen would be the damage integrator. The latter was accomplished by generating allowables from specimen tests in which loads were applied in simulated flight-by-flight sequences as random half cycles. These sequences were developed to simulate transport lower wing structure load histories.

For the sequence model, certain statistical parameters of the simulated stress sequence were chosen for the characterization of the fatigue behavior of the specimens. They are: 1) σ^2, mean square value of flight stresses about the flight one-g stresses, 2) $\bar{f}_{1g}$, mean of the flight one-g stresses, 3) $\bar{f}_{\min}$, mean of the minimum stress (usually

Fig. 1 Segment of test load sequence 24.

representing ground stresses for transport lower wing structure outboard of landing gear), and 4) $\bar{n}$, mean number of stress cycles per flight. During the course of the investigation, it was necessary to limit the scope of the experimental phase. As a result, the f_{min} stress level was held constant for all flight-by-flight tests. Once the fatigue allowable, N, is correlated with the remaining parameters, the damage for any given sequence can be found in one of two ways: 1) by summing damage due to each flight-by-flight segment in the sequence, each segment being identified with a given combination of sequence parameters, or 2) by computing the parameters for the entire sequence as a whole and determining the associated N. The latter approach was used in this investigation as it would be applicable to preliminary design.

An integral part of the cycle-by-cycle model is the cycle counting technique. A counting technique is applied to the flight-by-flight sequences to obtain occurrences of the individual cycles (defined according to the counting technique) comprising the sequences. These data along with the test lives are used to develop the model so described in a later section of this paper.

Flight-by-Flight Simulation and Test Program

Simulation Program

The hypothesis being tested in this investigation is that a viable damage model can be formulated based on fatigue test data where variable amplitude flight-by-flight loads are applied to the material specimen. This requires a procedure for generating test load sequences which simulate the loads environment encountered in service.

The service life of operational aircraft may span many years. To apply a real-time history of loads to laboratory test specimens would be costly and time consuming. Three common techniques[3] used to compress a load history for laboratory simulation are 1) to apply cyclic loads in test at a frequency higher than would be experienced in service, 2) to delete time at constant load, and 3) to omit certain variable loadings.

A 5 Hz test frequency was selected for the present investigation based on a previous observation[3] that only a small effect of test frequency was evident on fatigue life, and a small but unsystematic effect was observed[4] on macroscopic crack propagation life for tests conducted at frequencies of 0.1, 1, and 10 Hz.

Tests were performed to evaluate the influence on test life of deleting time at constant loading from a load history that contains high tensile loads which induce beneficial macro residual stresses. Load time-dependent relaxation of residual stresses[5] occurred when representative compressive loads were held for 24 hr on aluminum specimens. This relaxation significantly reduced the benefits of compressive residual stresses on test life. Based on these test results and the arguments presented earlier, it was decided to clip high tensile loads that would produce significant local yielding. Since these loads were omitted, provisions for including simulated ground hold periods in test sequences were not included. Likewise, compressive loads that would induce significant local yielding were to be clipped because relaxation of the resulting tensile residual stresses may also occur.

In Refs. 3 and 6, it was indicated that alternating taxi loads could be omitted from a simulation sequence without significantly influencing test life. However, it was recommended[3] that the minimum ground load be retained

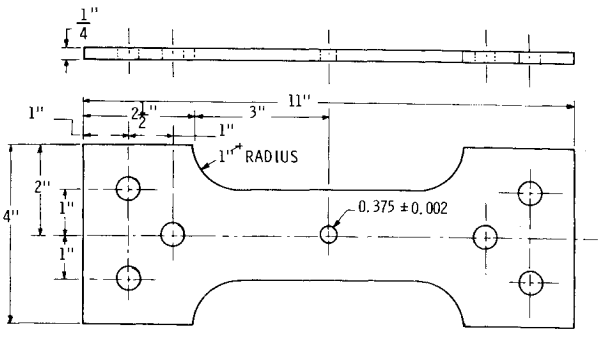

Fig. 2 Fatigue test specimen.

for simulating the ground portion of the ground-air-ground (GAG) cycle. Based on these studies, the simulation program was constructed such that only a minimum ground load would be inserted between flights. Besides omitting taxi loads, many of the smaller variable amplitude flight loadings were also deleted. The rationale for this deletion is presented later in this section.

A digital program[7] was developed to generate flight-by-flight sequences as a series of peak and valley loads on a digital computer such that a sequence contained over 300,000 independent cycles. The flights were constructed such that a load greater than the mean flight load was followed immediately by a load less than the mean flight load, but not necessarily of equal magnitude, and in turn by a load greater than the mean flight load until n-1 flight cycles had been generated. After n-1 flight cycles, a peak load equal to the mean flight load was inserted followed by a minimum ground load and then the following flight. For each flight in the load sequence, a load spectrum, 1-g mean load, f_{min}, and number of cycles per flight were assigned. Each of these parameters were specified or chosen at random from a distribution of values. The resulting load sequences were written on digital magnetic tapes.

Test Program

Flight loads data[8] for vertical center of gravity acceleration were used in establishing a baseline loading spectrum consisting of positive and negative incremental load factor, Δg, exceedance curves. The baseline spectrum as well as other spectra were a source of input information to the sequence generation program. In Ref. 8, the flight loads data were reduced to occurrences of Δg amplitudes using a primary peak count method. The digital program had been developed to construct flights consistent with the information provided by this reduction method.

To interface with the test facility a digital sequence was converted to a continuous analog signal (see sample, Fig. 1) by fitting half sine waves between the digital peaks and valleys. The signal was recorded on FM tape, and the tape was used on playback to drive electro-hydraulic closed-loop testing machines.

The specimens to which the flight-by-flight sequences were applied have the geometry shown in Fig. 2. The theoretical K_t of the specimen was 2.54 based on net section stresses and the specimen material was 7075-T651 aluminum.

Automatic counters were used during test to count the number of occurrences of the ground minimum load (also gives the number of flights). The mean life of the specimens for a particular test was computed using the flight cycle counter information. The digital tape containing the sequence for that test was then reduced to obtain peak and valley test loads by flight type (defined by a given f_{1g} value) from the beginning of the sequence to the mean test life. Bivariate tables of the peak and valley test load occurrences were produced for each of two alternative counting techniques. Technique A paired consecutive

Table 1 Bivariate table of cyclic load occurrences

Δg	0	0.25	0.35	0.45	0.55	0.65	0.75	0.85	0.95	1.05
−0.05	12546	112971	109							
−0.25		97906	39407	1710	77	18				
−0.35		2189	20275	5567	668	97	9	3	1	
−0.45		52	3001	2120	337	70	10	4		
−0.55		7	683	592	114	21	2			
−0.65			201	135	26	8				
−0.75		2	68	54	7	1				
−0.85			14	16						
−0.95			1	5						
−1.506		9	2026	5286	2733	1423	578	209	117	165

Table 2 Flight load spectra for preliminary tests

Δg	Spectrum 2a Σ (Δg) 2000 flights	Spectrum 2 Σ (Δg) 2000 flights	Spectrum 2b Σ (Δg) 2000 flights	Spectrum 2c Σ (Δg) 2000 flights
0.15	224000			
0.25	48000	48000	48000	48000
0.35	14000	14000	9432	18589
0.45	3560	3560	2353	4742
0.55	1070	1070	680	1427
0.65	428	428	252	569
0.75	178	178	77	234
−0.05	224000	48000	48000	48000
−0.15	184000			
−0.25	28000	28000	28000	28000
−0.35	5800	5800	11006	612
−0.45	1180	1180	2242	121
−0.55	320	320	606	34
−0.65	88	88	164	12
−0.75	28	28	49	6
−0.85	7.2	7.2	9	4
−0.95	2	2	2	2

for a test were established from these records and the specimen cross-sectional area.¶

Specimen surface crack length was measured from the edge of the circular hole during test using a calibrated low power microscope. Crack length measurements along with the number of flights applied at the time of each measurement were recorded. In general, crack growth was observable at the surface only during the latter 10% of the cyclic life to specimen rupture. In this paper, test lives are reported in terms of number of flights (or cycles) to specimen rupture.

Having established a baseline spectrum, preliminary flight-by-flight tests were performed to investigate the effect on test life of omitting small Δg values from the spectrum. In investigating the effect of omitting these values, large positive Δg values were clipped to a maximum value such that significant notch yielding did not occur. Two sequences were developed using load spectra 2a and 2 of Table 2. Spectrum 2a was the baseline spectrum. Spectrum 2 was obtained by omitting occurrences of Δg in the ranges $0.1 \leq |\Delta g| < 0.2$ from spectrum 2a. During these

Table 3 Test results for low load spectrum truncation investigation

Test number	Spectrum	$\bar{f}_{1g}$ Desired	$\bar{f}_{1g}$ Actual	$\bar{n}$	$\bar{f}_{min}$	Specimens per test	Mean test life
R1	2a	17.5 KSI	17.85	113	−8. KSI	6	6622 flights
R3	2	17.5	17.88	25	−8.	5	7975

Table 4 Test results for mean square value investigation

Test number	Spectrum	$\bar{f}_{1g}$ Desired	$\bar{f}_{1g}$ Actual	$\bar{n}$	$\bar{f}_{min}$	Specimens per test	Mean test life	Normalized
R3	2	17.5	17.88 KSI	25	−8. KSI	5	7975 flights	1
R7	2b	17.5	18.133	25	−8. KSI	6	7664	0.961
R8	2c	17.5	17.783	25	−8. KSI	6	7210	0.904

flight peak and valley loads. In addition, a peak-to-peak GAG cycle was defined for each flight by pairing the maximum flight load with the minimum ground load. Technique C§ paired the highest peak flight load with the ground minimum load, the second highest peak flight load with the lowest valley flight load, the third highest load was paired with the second lowest load and so forth until n flight cycles were defined for the flight. The technique was repeated for consecutive flights. An illustration of the test loads is given in Table 1 for Test No. 10 by counting Technique C. The actual ground minimum and flight mean loads were obtained for each test using strip chart recordings made during the test. The actual f_{1g} and f_{min} tests, n and f_{1g} were constant for each flight in a sequence. The test conditions and test results are given in Table 3 for Tests $R1$ and $R3$.

Omitting Δg values in the ranges $0.1 \leq |\Delta g| < 0.2$ resulted in approximately a 20% increase in test life on a flight basis. However, Test No. R1 required approximately 3.75 times as many cycles to failure as compared to Test R3. In order to remain within the scope of the experimental phase, it was necessary that for further tests Δg values in these ranges be omitted.

§A third technique, Technique B, was also used in Ref. 7 but was not required in this paper.

¶Because of error in the bias voltage used in the test machine load controller, the desired and actual specimen loads were not always the same. When this occurred, actual loads were related to desired loads in the following way: $(f_{1g})_{ac} = x + y$, $(f_{min})_{ac} = xZ_d + y$, and $f_{ac} = x(1 + \Delta g) + y$ where x and y are scale parameters. For all tests, $(f_{min})_{ac} = -8$ KSI net section stress.

Table 5 Cumulative frequency distributions of load spectra

Δg	Spectrum 1	Spectrum 2	Spectrum 3
0.25	1.000	1.000	1.000
0.35	0.1875	0.2917	0.4583
0.45	0.0375	0.07417	0.2083
0.55	0.01146	0.02229	0.1042
0.65	4.583×10^{-3}	8.917×10^{-3}	0.04583
0.75	2.083×10^{-3}	3.708×10^{-3}	0.02292
0.85	$1. \times 10^{-3}$	1.625×10^{-3}	0.01042
0.95	$5. \times 10^{-4}$	9.167×10^{-4}	4.792×10^{-3}
1.05	2.5×10^{-4}	5.417×10^{-4}	2.292×10^{-3}
1.15	1.458×10^{-4}	3.333×10^{-4}	1.125×10^{-3}
−0.05	1.000	1.000	1.000
−0.25	0.5833	0.5833	0.5833
−0.35	0.075	0.1208	0.1583
−0.45	0.0125	0.02458	0.04583
−0.55	3.125×10^{-3}	6.667×10^{-3}	0.0142
−0.65	8.333×10^{-4}	1.833×10^{-3}	4.167×10^{-3}
−0.75	2.292×10^{-4}	5.833×10^{-4}	1.208×10^{-3}
−0.85	6.875×10^{-5}	1.5×10^{-4}	3.75×10^{-4}
−0.95	2.083×10^{-5}	4.167×10^{-5}	1.042×10^{-4}

Table 6 Maximum load levels

Desired f_{1g}	Maximum Load, g
14.5	2.15
15.8	2.05
16.5	1.95
16.6	1.95
17.5[a]	1.85
18.5	1.75

[a] Tests R1, R3, R7, and R8 were truncated at 1.75g.

Additional preliminary tests were conducted to evaluate the sufficiency of the σ^2 parameter as providing the measure of the intensity of the cyclic flight loads. For the same σ^2 value there exists any number of load spectra. If σ^2 were to be a sufficient parameter for the sequence model then sequences based on alternative spectra having the same mean square value should produce similar test lives. The σ^2 value of Δg was computed for spectrum 2. Two alternative spectra of different shape were then defined to have the same σ^2 value. These spectra are identified as 2b and 2c in Table 2. Test sequences were generated using these spectra and applied to test specimens. The f_{1g} and n were constant for each flight in these sequences. The test conditions and results are given in Table 4. Based on these test results, the σ^2 parameter was confirmed as providing a measure of flight load intensities.

A series of tests were then conducted to establish an initial data base for developing empirical damage models. During these tests, either f_{1g}, n, or the load spectrum was changed from one test sequence to another and each was constant for every flight within a sequence. To provide a range of flight loading intensities for these tests, two additional load spectra were developed. These spectra along with spectrum 2 are presented in a normalized form as cumulative frequency distributions in Table 5. When these spectra are superimposed on the 1-g mean flight load, a corresponding maximum possible load may occur. These maximum loads, expressed in terms of c.g. absolute acceleration, are given in Table 6 for each f_{1g} stress (the maximum loads in Table 6 apply to all test sequences). The test conditions and test lives for each of the data base tests (Test Nos. 10–19, 26, and 31) are given in Table 7.

Tests were also conducted wherein n varied from flight to flight within a sequence. Additional tests were conducted wherein all three parameters (n, f_{1g}, and the load spectra) were allowed to vary from flight to flight within a sequence. The test conditions are given in Table 8 and the test results in Table 9.

Table 7 Results of flight simulation tests for alternate loading sequences

Test no.	Spectrum	f_{1g} Desired	f_{1g} Actual	$\bar{n}$	$\bar{f}_{min}$	No. of specimens	Mean test life Flights	Mean test life Cycles
10	2	15.8	16.	25	−8.0	6	12546	313650
11	1	17.5	17.65	25	−8.0	6	9934	248350
12	1	15.8	15.933	25	−8.0	6	17604	440100
13	3	17.5	17.467	25	−8.0	6	4968	124200
14	3	15.8	15.85	25	−8.0	6	7675	191875
15	1	15.8	15.88	61	−8.0	5	8112	494832
16	1	17.5	17.75	61	−8.0	6	4394	268034
17	2	15.8	16.133	61	−8.0	6	6153	375333
18	3	15.8	16.167	61	−8.0	6	3195	194895
19	3	17.5	17.683	61	−8.0	6	1948	118828
26	2	16.6	16.883	25	−8.0	6	10932	273300
31	2	15.8	15.8	10	−8.0	2	27076	270760

Table 8 Probability of flight types comprising sequence by test number

Test no.	Possible n	Probability	Possible f_{1g}	Possible spectrum	Probability
21	25	0.5	15.8	1	0.7
				3	0.15
	61	0.5	17.5	1	0.1
				3	0.05
	10	0.4297			
22	25	0.5	15.8	2	1
	61	0.0703			
				1	0.075
			14.5	2	0.045
	10	0.243		3	0.030
24	19	0.437		1	0.35
	37	0.320	16.5	2	0.21
				3	0.14
				1	0.075
			18.5	2	0.045
				3	0.030

Damage Modeling Efforts

The relatively modest test program described in the previous section resulted in a consistent set of data from which two damage models were developed and evaluated. For the sequence model, the damage index, N, cycles to rupture, was expressed as a function of statistical parameters of the entire stress sequence. In the cycle-by-cycle model, the damage index, N, is the number of cycles to rupture of a specific stress cycle as defined by its mean and alternating net section stresses. In application, this method is analogous to the use of S-N data with Palmgren-Miner's linear damage theory. The damage ratios are summed linearly, however, the index N is generated from random flight-by-flight sequences where a counting technique becomes specifically associated with the index N. Then, more precisely, N is a statistical representation of the damage caused by a specific cycle among all other cycles from all sequences used as a data base.

Sequence Model

The functional form selected for the damage index, N, for the sequence model was

$$N = D(\sigma^2)^a(\bar{f}_{1g})^b(\bar{n})^c(1 - \bar{Z})^d \qquad (1)$$

Table 9 Test results for multiple flight simulation load sequences

Test no.	Spectrum	f_{1g} Desired	f_{1g} Actual	$\bar{n}$	$\bar{f}_{min}$	Number of specimens	Mean test life Flights	Mean test life Cycles
21	1, 3	16.06	16.02	43.186	−8.0	6	8421	363669
22	2	15.8	15.8	21.166	−8.0	3	14631	309675
24	1, 2, 3	16.5	16.5	22.456	−8.0	6	11063	248429

where the statistical parameters (σ^2, $\bar{f}_{1g}$, $\bar{Z}$, and $\bar{n}$) were based on the entire stress sequence and the exponents and the constant D were to be determined. Since f_{min} was constant for every sequence in the present investigation, the last factor in Eq. (1) merely provided a more complicated functional dependence on f_{1g}. Thus, for this investigation, the last factor was eliminated (i.e., exponent d was set equal to zero).

The functional form, Eq. (1), was chosen because of its simplicity and a lack of any a priori knowledge of the dependence of a damage index on sequence statistical parameters. Further, it was thought that this relatively simple form would amply demonstrate the feasibility of damage calculations based on flight sequences.

Taking the logarithm of Eq. (1), recalling that $d = 0$, results in

$$\log N = \log D + a \log (\sigma^2) + b \log (\bar{f}_{1g}) + c \log (\bar{n}) \quad (2)$$

Using the measured value of N, cycles to failure, for each individual specimen subjected to one of the load sequences $R3$, 10–19, 26, or 31 and using the appropriate sequence statistics, one can find a best fit for log D, a, b, c by the method of least squares. The result is

$$N = 5.0737 \times 10^8 (\sigma^2)^{-2.114} (\bar{f}_{1g})^{-0.61492} (\bar{n})^{0.12431} \quad (3)$$

for $\bar{f}_{1g} > 0$.

Cycle-by-Cycle Model

The functional form for the damage index N used in the cycle-by-cycle model is a common form used for presenting S-N data[9] in which lines for different constant cyclic mean stresses, f_m, are parallel straight lines on log-log plots of N vs alternating stress, f_a. This form is

$$(1/N) = \lambda \left(\frac{1 - \kappa f_m}{f_a} \right)^{\beta} \quad (4)$$

where λ, κ, and β are to be determined by the method of least squares. A word of caution in using Eq. (4) is in order. The constants λ, κ, and β are dependent on the counting technique used in establishing the occurrences of cycles of given f_m and f_a. Therefore, a similar counting technique should be used when estimating life using Eq. (4).

Equation (4) is nonlinear in β and κ thus an iterative nonlinear least squares technique was used to obtain values for λ, β, and κ. The expression for $(1/N)$ was approximated to include linear terms in λ, β, and κ to give

$$\frac{1}{N} \simeq \left(\frac{1}{N} \right)_{approx} = \lambda \left(\frac{1 - \kappa_0 f_m}{f_a} \right)^{\beta_0} + \log \left(\frac{1 - \kappa_0 f_m}{f_a} \right)^{\beta_0} (\beta - \beta_0) - \lambda_0 \beta_0 \frac{f_m}{f_a} \left(\frac{1 - \kappa_0 f_m}{f_a} \right) (\kappa - \kappa_0) \quad (5)$$

and the optimization used was

$$\frac{\partial}{\partial(\lambda, \beta, \kappa)} \left\{ \sum_{\text{sequences}} \left[\sum_{\text{cycles}} \left(\frac{n_i}{N_{approx}} \right) - 1 \right]^2 \right\} = 0 \quad (6)$$

where initial values for β_0 and κ_0 are estimated and input and the initial value for λ_0 is subsequently calculated using the linear least squares method. The n_i are the number of occurrences of cycles having the ith combination of f_m and f_a. The optimization process of Eq. (6) yields three linear equations in the three unknowns λ, β, and κ. These three equations are solved. If any of the three test conditions listed below were violated, the iterative procedure was repeated with the solved values of λ, β, and κ replacing λ_0, β_0, and κ_0, respectively.

$$|(\lambda - \lambda_0)/\lambda_0| < 10^{-6} \quad (7)$$

$$|(\beta - \beta_0)/\beta_0| < 10^{-6} \quad (8)$$

$$|(\kappa - \kappa_0)/\kappa_0| < 10^{-6} \quad (9)$$

The cycles summed over were the loading cycles corresponding to mean rupture life of all specimens tested to the same sequence. The optimization determines λ, β, and κ such that all the sequences used in the data base (Test Nos. R3, 10–19, and 26) result in a damage summation as close to one as possible in the least-squares sense. The resulting cycle-by-cycle model is

$$\frac{1}{N} = 2.3836 \times 10^{-9} \left(\frac{1 - 0.030638 f_m}{f_a} \right)^{-3.105} \quad (10)$$

Model Evaluation

An evaluation of the developed models is made by comparing predicted with mean test lives. The comparison also includes predicted lives using the Palmgren-Miner linear damage theory with constant amplitude based fatigue allowable data.

For the sequence model, predicted lives were obtained using Eq. (3). The peak and valley flight test loads (up to the mean test life) and the actual $\bar{f}_{1g}$ applied in test were used to calculate the σ^2 value. The $\bar{f}_{1g}$ and $\bar{n}$ values were known from the test conditions with the exception of Tests 21, 22, and 24. For these tests, $\bar{n}$ was obtained by dividing the cyclic test life by the test life in flights where the cyclic test life was obtained by counting the cycles from the digital tape (up to the mean test life in flights). The $\bar{f}_{1g}$ for Tests 21 and 24 was computed as the average of the corresponding values for every flight in the sequence. In predicting fatigue life of specimens in Test No. $R1$, certain corrections were required. The test sequence for this test included loads in the ranges $0.1 \leq |\Delta g| < 0.2$ with 113 load cycles per flight. The damage model, however, was based on test results when these low loads were omitted. Thus, the σ^2 for this test sequence was computed after omitting the low loads and using $\bar{n} = 25$. The resulting predicted cyclic life was multiplied by the factor 113/25 to yield an estimate of the cyclic life when the low loads are present.

For the cycle-by-cycle model of Eq. (10), a computer program was developed[7] to sum the damage ratios n_i/N for each group of cycles of a given f_a and f_m. Input data consisted of bivariate tables of the peak and valley loads obtained using counting Technique C together with the $\bar{f}_{1g}$ for each flight type and each test. The output is the damage summation.

Using constant amplitude S-N data and the Palmgren-Miner damage theory, a predicted cyclic life, N', was computed using the equation

$$\log N' = \frac{\log f_a - 2.218 - 0.018 f_m + 0.00046 f_m^2}{-0.249 - 0.0055 f_m + 0.000097 f_m^2} \quad (11)$$

Table 10 Comparison of predicted to test life for different models

Test no.	Mean test life cycles	Sequence model $\frac{n}{N}$	Cycle-by-cycle $\sum\frac{n}{N}$	Linear damage $\sum\frac{n}{N}$
R1	748286	0.860	1.224	1.166
R3	199375	0.966	1.076	1.195
R7	191600	0.955	1.018	1.134
R8	180250	1.086	1.005	1.091
10	313650	1.031	0.931	1.298
11	248350	1.04	1.03	1.234
12	440100	0.96	1.059	1.539
13	124200	0.946	1.024	1.034
14	191875	0.975	0.917	1.158
15	494832	0.965	0.961	1.104
16	268034	1.051	0.993	0.895
17	375333	0.937	0.982	1.059
18	194895	0.999	0.924	0.876
19	118828	1.06	0.988	0.73
26	273300	0.919	1.077	1.357
21	363669	0.970	1.023	1.157
22	309675	1.064	0.909	1.335
24	248429	1.039	1.026	1.275
31	270760	1.109	1.038	1.874

where f_a and f_m are given in KSI for gross section stresses. Equation (11) was obtained by curve fitting[7] constant amplitude S-N data from Ref. 10. A constant amplitude test of four specimens was made for the purpose of scaling the S-N data to make it applicable to the specimen used in this investigation. The scaling relation used was $N = N'/1.36337$ where N' is as calculated from Eq. (11). Predicted lives were obtained using the bivariate table of peak and valley loads obtained using counting Technique C.

The predicted lives are compared to test lives in Table 10 using the test results from Tables 3, 4, 7, and 9. The values in the table are the ratios of actual test lives to predicted lives. Values greater than one indicate the prediction underestimated the actual life and values less than one indicate an overestimation of life. The striking feature of the values in Table 10 is the consistency of the predictions using the proposed methods. A measure of this consistency is the unbiased standard deviation of the 19 values in each column. The deviations for the sequence and cycle-by-cycle models are 0.0641 and 0.0728, respectively, while the deviation for the linear damage model is 0.2495. This comparison is dramatically illustrated by normal distribution curves fitted to the data in Table 10 as shown in Fig. 3.

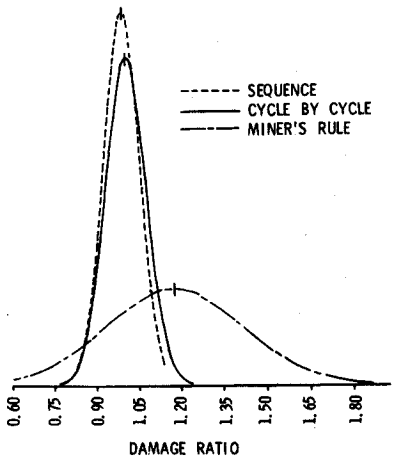

Fig. 3 Damage model comparison—a normal distribution fit of predicted lives.

The proposed models did remarkably well in predicting specimen fatigue life in every case except for Test R1. For this test it must be pointed out that 80% of the peak and valley loads occurred in the ranges $0.1 \leq |\Delta g| < 0.2$. Both damage models were developed from test results wherein these low loads were omitted. Yet, a comparison of results from Tests R1 and R3 show that these low loads do contribute to damage. The sequence model predicts a longer life than the actual life and the cycle-by-cycle model underestimates life for Test R1. It appears that the cycle-by-cycle model attributes too much damage to these low loads. This aspect of the model will be discussed further in the next section.

The Palmgren-Miner damage theory gave inconsistent and usually inaccurate results. It will be shown through additional analysis using the test results and the cycle-by-cycle model that the linear theory and S-N data attribute too much damage to the GAG cycles. A measure of the influence of the GAG cycle on the total damage calculation for a sequence was provided by a study of data from the paired tests (12,15), (10,17), (11,16), (14,18), and (13,19). The load sequences for the tests in each pair differed only in the flight length; that is, the parameter n was either 25 or 61 cycles per flight. Assuming that the flight cycle damage and GAG cycle damage are directly additive, the damage due to each source can be combined as follows:

$$\text{PDGAG}(I) + \text{PDFLT}(I) = 1 \quad I = \text{Tests } 12,10,11,14,13 \tag{12a}$$

$$\text{PDGAG}(J) + \text{PDFLT}(J) = 1 \quad J = \text{Tests } 15,17,16,18,19 \tag{12b}$$

where PDGAG *(I)* is the part damage due to all GAG cycles in Test I and PDFLT *(I)* is the part damage due to all flight cycles in Test I and similarly for PDGAG *(J)* and PDFLT *(J)*. For each pair of Tests I and J the following relationships hold:

$$\text{PDGAG}(J) = 1.2\,A(I,J)\ \text{PDGAG}(I) \tag{13a}$$

$$\text{PDFLT}(J) = B(I,J)\ \text{PDFLT}(I) \tag{13b}$$

where $A(I,J)$ is the ratio of the number of flights (and, hence, GAG cycles) for Test J to the number of flights for the paired Test I, and similarly, $B(I,J)$ is the ratio of flight cycles. The factor 1.2 was inserted to account for the possible increase in severity of the GAG cycle damage in the longer flights due to the increased occurrences (by percentage on a flight basis) of high peak loads per flight. This factor was established, in part, using linear damage theory and Eq. (11). The values of PDGAG*(I)* and PDGAG*(J)* are not particularly sensitive to the value of the factor selected from a reasonable range. Equations (12) and (13) are combined to yield two equations in two unknowns

$$\text{PDGAG}(I) + \text{PDFLT}(I) = 1 \tag{14a}$$

$$1.2\,A(I,J)\ \text{PDGAG}(I) + B(I,J)\ \text{PDFLT}(I) = 1 \tag{14b}$$

Table 11 shows a comparison of the GAG cycle damage computed from test results (i.e., solution of Eqs. (14) and referred to as the sequence calculation) with that computed from linear damage theory, S-N data and a once per flight peak-to-peak GAG cycle definition. Counting Technique A was used for the damage ratio calculations using the linear theory. The sequence calculated damages for Tests 13 and 19 resulted in a negative damage for the GAG cycles. These values were set equal to zero.

The predicted damage for the peak-to-peak GAG cycle definition overestimates, by factors ranging from 2 to greater than 10, the GAG cycle damage obtained from the experimental results. This overestimation may account for some of the errors when the linear damage theory is applied to flight-by-flight load sequences. Predicted test lives would be conservative for specimens subject to

Table 11 Ground-air-ground cycle damage to total damage ratios

Test no.	Spectrum	$\bar{f}_{1g}$	$\bar{n}$	Mean test life Cycles	Flights	Sequence calculation	Peak to peak
12	1	15.93	25	440100	17604	0.254	0.737
15	1	15.88	61	494832	8112	0.140	0.574
10	2	16.	25	313650	12546	0.354	0.721
17	2	16.13	61	375333	6153	0.208	0.553
11	1	17.65	25	248350	9934	0.184	0.710
16	1	17.75	61	268034	4394	0.097	0.537
14	3	15.85	25	191875	7675	0.075	0.695
18	3	16.17	61	194895	3195	0.038	0.521
13	3	17.47	25	124200	4968	0	0.665
19	3	17.68	61	118828	1948	0	0.481

flight-by-flight sequences containing short flights as in Test 31 of Table 10. Predicted lives would be expected to be unconservative for sequences containing flights with larger n values such as in Tests 16 and 18. These observed trends indicate that predicted lives would be expected to be even more unconservative for values of n much larger than used in this investigation.

To gain further insight into the behavior of the linear theory, the cycle-by-cycle model results were compared to the linear theory as in Fig. 4. Here, the allowables from the cycle-by-cycle model are determined by Eq. (10) converted to a gross section stress basis, i.e.,

$$\frac{1}{N} = 4.5419 \times 10^{-9} \left(\frac{1 - 0.037708\, f_m}{f_a} \right)^{-3.105} \qquad (15)$$

and appears as solid lines in Fig. 4. The linear damage theory S-N curves, Eq. (11), are shown as dashed lines. The curves obtained from Eq. (15) illustrate a much larger percentage difference in N for different f_m values (for a given f_a value) than the curves of Eq. (11). This influence of f_m on N indicates that a higher percentage of total damage is attributed to flight cycles than implied by the linear damage theory and Eq. (11).

Discussion

The preceding section presents damage models which appear to be attractive alternatives to the Palmgren-Miner theory for accurately estimating fatigue lives of aluminum specimens. It is important to digress a bit here to discuss why these more complicated models are needed and how they account for material defects and load interaction effects. We further suggest the need for additional work.

The developed models were based on tests wherein the test specimen performed the damage integration process at the micro level. At this level, material and fabrication defects exist in the material[11] adjacent to the notch. An attractive hypothesis of the integration process would consist of strain accumulation through microcrack formation and extension due to both the higher and lower loads within a load sequence. However, the rate of strain accumulation is changed caused by load interaction effects and microcrack length. The larger amplitude loads within a sequence cause localized plastic deformation.[11] Load interaction effects would arise at a localized site for the case where the surrounding structure was elastically deformed. Upon changing to lower amplitude load levels residual stresses[11] would exist at the interface zone between the defect and surrounding structure. These stresses would interact with smaller amplitude flight load cycles by lowering the mean stress level of these cycles at the plastic interface zone of the defect. Consequently, the rate of strain accumulation would be less for the smaller load cycles that followed a high load than for those that preceded the high load. The smaller load cycles in turn would tend to

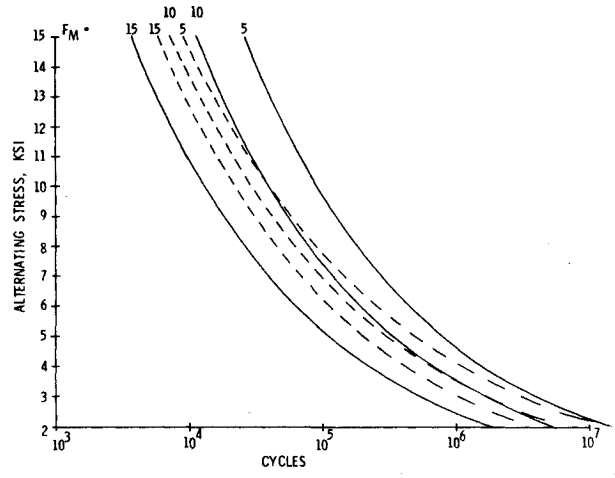

Fig. 4 Comparison of fatigue allowables for the cycle-by-cycle model vs constant amplitude.

relax the residual stress by microcrack extension into the interface zone. Interaction effects would arise also from the ground minimum load that followed a previous high flight load. The effect of this interaction would be to reduce the magnitude of the existing compressive residual stress or induce a tensile residual stress, upon unloading, at the interface zone. In either case the effective mean stress level of the following flight load cycles would be higher and produce an increase in the strain accumulation rate as compared to the rate for similar cycles that preceded the ground loading. In addition to changes in the strain accumulation rate due to load interaction effects, the rate would also be influenced by increasing microcrack length due to crack extension and the coalescing of two or more crack nuclei.

The strain accumulation rate could change frequently as in the tests reported in this paper since the large and small load amplitudes were continuously changing in the simulated flight-by-flight load sequences. Several specimens were tested to each sequence so that a number of defects and the response of these defects under cyclic loads were represented in the data base used for model development. For these reasons, the models were considered to statistically account for defects and load sequence effects during the formation and coalescing of crack nuclei when forming a predominant propagating macroscopic crack. Also included was the crack propagation phase.

Load interaction influences upon damage integration were limited to the micro level since clipping of maximum load levels was performed such that significant notch yielding did not occur during test. The effect of even higher loads that could occur infrequently would be to induce macro yielding of the notch material. This yielding causes macro residual stresses to be induced upon unloading[12] These latter stresses would set the stage for additional load interaction effects on fatigue life. One important effect is the relaxation of residual stresses as a result of further cyclic loading[12] and sustained loads.[5] The results of a simple test program outlined in Ref. 5 suggest that the beneficial effects of overloads on aircraft (due to induced residual stresses) can be significantly reduced overnight. The implication is that two modeling efforts are necessary in formulating a life prediction methodology, 1) damage modeling, such as suggested in the previous section, and 2) residual stress relaxation modeling to account for the effects of macro residual stresses on notch cyclic stress levels.

A more extensive data base would be necessary before general application could be made of the models developed in this investigation to aircraft structure analysis. The sequence model was developed for preliminary design purposes. Life predictions can be easily obtained without

defining cycles and performing damage summation on a cycle-by-cycle basis. But, accompanying this ease of application, one would expect a decrease in accuracy for a wide range of stress spectra. Thus, additional tests may be necessary to, 1) include f_{min} as an additional parameter, 2) include provisions for assessing alternate structure details, and 3) further investigate the functional form of Eq. (11). Regarding the latter aspect, the percentage change of N with $\bar{n}$ appears to be a function of σ^2 whereas the selected functional form of N cannot account for this change.

The cycle-by-cycle model also requires further work. This model apparently attributes too much damage to the individual 0.15 Δg alternating load cycles for the specimens used in this investigation. This may be caused by the fact that the main contribution of these cycles was their interaction with larger amplitude cycles. A large percentage of cyclic loads for the sequence of test R1 were in the ranges $0.1 \leq |\Delta g| < 0.2$. Hence there were portions of the sequence which contained several 1.15 g to 0.85g load cycles adjacent to each other. It is possible that the cycles interior to this string of cycles are less damaging than the cycles which interact with larger amplitude cycles. If this is the case, the damage summation is nonlinear. Collecting the data base near or below the lowest truncation level anticipated (or at a truncation level below which no appreciable shortening of life occurs in terms of flights) may minimize this potential source of error as the nonlinearities would to some extent be averaged out. Another obvious need is for additional tests to include provisions for modifying Eq. (10) to handle various structural details and materials.

The methodology as developed in this paper for establishing a cycle-by-cycle model can potentially provide an economic savings, in addition to consistent life prediction accuracy for variable load sequences, over the characterization of a new material or structure specimen using conventional constant load amplitude tests. It is anticipated that fewer tests would be required to fit the constants in the cycle-by-cycle model as compared to the number of tests for constant amplitude characterization.

Conclusion

The results of this investigation have demonstrated that it is feasible and desirable to develop test integrated damage models. The two models developed herein have shown marked improvement over the Palmgren-Miner Theory in consistently predicting specimen life accurately when the loading simulates flight-by-flight aircraft load cycles. It is recommended that the modeling efforts be extended to apply to more complex specimens or components and other materials.

References

[1]Miner, M. A., "Cumulative Damage in Fatigue," *Journal of Applied Mechanics,* Vol. 12, No. 3, Sept. 1945, pp. A-159–A-164.

[2]Reimann, W. H., "Some Metallographic Observations of Cumulative Damage in Fatigue," AFML TR 68-359, Dec. 1968, Air Force Materials Lab., Wright-Patterson Air Force Base, Ohio.

[3]Schijve, J., Broek, D., DeRijk, P., Nederveen, A., and Sevenhuysen, P. J., "Fatigue Tests With Random and Programmed Load Sequences, With and Without Ground-to-Air Cycles. A Comparative Study on Full-Scale Wing Sections," AFFDL TR 66-143, Oct. 1966, Air Force Flight Dynamics Lab., Wright-Patterson Air Force Base, Ohio.

[4]Schijve, J., "Effects of Test Frequency on Fatigue Crack Propagation Under Flight-Simulation Loading," NLR MR 72010, April 1972. National Aerospace Lab., Amsterdam, The Netherlands.

[5]Simpkins, D., Neulieb, R. L., and Golden, D. J., "Load-Time Dependent Relaxation of Residual Stresses," *Journal of Aircraft,* Vol. 9, No. 12, Dec. 1972, pp. 867–868.

[6]McCulloch, A. J., Melcon, M. A., Crichlow, W. J., Foster, H. W., and Rebman, R., "Investigation of the Representation of Aircraft Service Loadings in Fatigue Tests," ASD TR 61-435, Jan. 1962, Aeronautical Systems Division, Wright-Patterson Air Force Base, Ohio.

[7]Neulieb, R. L. and Simpkins, D., AFFDL TR, Air Force Flight Dynamics Lab., Wright-Patterson Air Force Base, Ohio, to be published.

[8]Clay, L. E., Strohm, J. A., Silcott, C. J., and Nash, J. F., "C-130 VGH Flight Loads Program (1968–1970)," 70WRNE-199, 1970. Warner Robins Air Material Area, Robins Air Force Base, Ga.

[9]Sorensen, A., Jr., "A General Theory of Fatigue Damage Accumulation," *Journal of Basic Engineering, Transactions of the ASME,* March 1969, pp. 1–13.
ASME, Vol. 91, Ser. D, March 1969, pp. 1–13.

[10]Crichlow, W. J., McCulloch, A. J., Young, L., and Melcon, M. A., "An Engineering Evaluation of Methods for the Prediction of Fatigue Life in Airframe Structures," ASD TR 61-434, March 1962, Aeronautical Systems Div., Wright-Patterson Air Force Base, Ohio.

[11]Grosskreutz, J. C., "Fatigue Mechanisms in the Sub-Creep Range," *Metal Fatigue Damage—Mechanisms, Detection, Avoidance, and Repair,* ASTM STP 495, 1971, pp. 5–60, American Society for Testing and Materials, Philadelphia, Pa.

[12]Impellizzeri, L. F., "Cumulative Damage Analysis in Structural Fatigue," *Effects of Environment and Complex Load History on Fatigue Life,* ASTM STP 462, 1970, pp. 40–68, American Society for Testing and Materials, Philadelphia, Pa.